

## Growth retardation of diflunisal in antisolvent crystallization

Ka-Ram Kwon and Sang-Do Yeo<sup>†</sup>

Department of Chemical Engineering, Kyungpook National University, Daegu 41566, Korea

(Received 25 August 2017 • accepted 2 February 2018)

**Abstract**—Diflunisal, an analgesic anti-inflammatory drug, was recrystallized from acetone solution using water and carbon dioxide as antisolvents. The crystallized diflunisal showed an acicular crystal habit with a very high aspect ratio. Growth retardation of diflunisal crystals was observed when ultrasound was added during the recrystallization and when habit-modifying agents were applied to the system. For example, an increase in sebacic acid concentration from 0.229 to 2.132 wt% lowered the aspect ratio of the crystal from 62 to 8.5, while an increase in Span 83 concentration from 1.712 to 4.415 wt% reduced the aspect ratio from 11 to 4.0. Differential scanning calorimetry and X-ray diffraction analysis revealed that the presence of ultrasound and habit-modifying agents may induce structural modifications as well as the growth retardation of diflunisal crystals.

Keywords: Antisolvent, Diflunisal, Growth Retardation, Recrystallization, Ultrasound

### INTRODUCTION

Antisolvent crystallization has been commonly applied for the crystallization of a number of pharmaceutical compounds [1-4]. Major advantages of antisolvent crystallization include the easy handling of difficult-to-comminute materials (e.g., pharmaceuticals), lack of heating and cooling steps that can cause thermal degradation, and use of nontoxic antisolvents such as water and carbon dioxide. There are two main objectives in the application of antisolvent crystallization to pharmaceutical compounds: micronization of particles, and modification of external crystal habits. Micronization reduces the particle size, while increasing the particle surface area to enhance solubility and bioavailability. Modification of the external habit is carried out to improve downstream processes such as transportation, manufacturing, and long term storage. We chose to modify the crystal external habit of a pharmaceutical compound based on the variation of several crystallization experimental variables.

In antisolvent crystallization, a solute (drug compound) is precipitated out of solution when the solution and the antisolvent are rapidly mixed. This procedure induces a large supersaturation of the solution and also leads to an extremely high rate of nucleation and crystal growth. Because of these effects, antisolvent crystallization tends to produce particles with an acicular (needle-like) crystal habit. This is caused by rapid crystal growth along a given axial direction, resulting in the production of particles that have a very large aspect ratio. This phenomenon was observed in our previous study, in which caffeine was crystallized using a carbon dioxide antisolvent to give needle-like crystals [5].

However, acicular crystals with a high aspect ratio are undesirable because they have poor powder flow properties, poor filtration

characteristics, a tendency to cake, and are often brittle. Thus, several technologies have been adopted to prevent the formation of acicular crystals, including 1) The use of different solvents or antisolvents, 2) Crystallization using lower levels of supersaturation, 3) Change in experimental variables, 4) Application of external disturbances such as ultrasound, and 5) The addition of habit-modifying agents or growth retardants. For example, the use of different solvents and antisolvents changes the environment of nucleation and crystal growth, and will affect the rate of crystal lattice formation at the interface of the crystal surface and solution, thus potentially changing the crystal habit of the final product. In addition, crystallization using lower levels of supersaturation decreases the driving force of mass transfer, and can reduce the abnormally fast growth of a crystal surface. Furthermore, altered process conditions such as temperature, concentration, and mixing rate of solvent and antisolvent may influence supersaturation and therefore modify the crystal habit. Moreover, the use of ultrasonic waves during the crystallization process reduces the width of the metastable zone and nucleation induction time, which can influence the properties of the resulting crystals. Finally, the addition of habit-modifying agents is perhaps the most powerful method for directly influencing the nucleation and crystal growth mechanisms of a target crystallizing material.

The main role of such a habit-modifying agent is to reduce the growth of a particular surface of the growing crystal, ultimately preventing the crystals from forming a needle-like habit. The effect of the habit-modifying agent on crystal growth is related to the strength of intermolecular bonds that form during the adsorption of the agent on the crystal surface. Chemical interactions that commonly occur at the crystalline interface during adsorption of the agent include van der Waals forces, ionic interactions, and hydrogen bonds [6]. If the resulting interactions are strong, the adsorbed agent will effectively disrupt the movement of crystallizing molecules, and influence the crystal growth rate. If the bonding is relatively weak, the agent is easily swept away from the surface and has a signifi-

<sup>†</sup>To whom correspondence should be addressed.

E-mail: syeo@knu.ac.kr

Copyright by The Korean Institute of Chemical Engineers.

cantly smaller effect on crystal growth retardation. It is therefore necessary to select the correct habit-modifying agent to reduce fast crystal growth and to prevent the formation of an acicular habit. The previous investigations on the effects of additives on the crystal shape and size can be found in the literature [7,8].

In this study, the crystal habit of diflunisal, an analgesic anti-inflammatory drug [9,10], was modified by performing antisolvent crystallization using water and carbon dioxide as antisolvents. The effects of habit-modifying agents on the growth retardation of the diflunisal particles were examined. The variations in particle size distribution and the change of aspect ratio of the diflunisal crystals were measured as functions of additive concentration.

## EXPERIMENTAL METHODS

### 1. Materials

Diflunisal (CAS 22494-42-4) and was purchased from Sigma Aldrich. Acetone was selected as the organic solvent to dissolve diflunisal. Distilled water and carbon dioxide were used as the liquid and supercritical antisolvents, respectively. Sebacic acid (CAS 111-20-6) and Span 83 (CAS 8007-43-0) were employed as habit-modifying agents. Table 1 shows the physicochemical properties of diflunisal.

### 2. Experimental Procedure

Antisolvent crystallization experiments were performed using two different antisolvents: water (liquid) and carbon dioxide (supercritical fluid). To apply these two types of antisolvent, different pieces of apparatus were required. The experimental apparatus used in the antisolvent experiments is well described in our previous publication [5], so a brief experimental procedure is given here. For the crystallization experiments, diflunisal was dissolved in pure acetone (0.06 g/mL). At this concentration, diflunisal is readily soluble in acetone. When habit-modifying agents were added to the experiments, the selected agent was dissolved in the diflunisal solution at concentrations of 0.2-4.3 wt%. At these concentrations, the mixture of acetone, diflunisal, and habit-modifying agent formed a clear single phase solution. For the water-antisolvent experiment, the prepared diflunisal solution (10 mL) was injected into the crystallizing vessel containing the antisolvent (water, 60 mL). As the solution was injected, the mixture of solution and antisolvent was

vigorously agitated allowing a prompt precipitation of diflunisal. Following solution injection, the system was continuously agitated to ensure sufficient crystal growth. In each experiment, the total time allowed for solution injection and crystal growth (crystal residence time in the system) was typically 10 min. To investigate the effect of ultrasound in the water-antisolvent experiments, ultrasonic waves (5 W power output) were applied to the system for 10 s during the solution injection step. For the carbon dioxide-antisolvent experiments, the diflunisal solution (10 mL) was loaded into the crystallizing chamber. Carbon dioxide was then injected into the chamber at a controlled rate to achieve mixing of the drug solution and antisolvent. During carbon dioxide injection, the pressure of the crystallizing chamber increased at 10.3 bar/min. This caused expansion of the solution and diflunisal nucleation. Following nucleation, the system was further pressurized to 95 bar until the carbon dioxide and solution phases were close to merging. At this stage, the crystallization process was assumed to be complete. The precipitated crystals fell to the bottom of the chamber and were collected using a metal filter. Finally, the crystallizing chamber was depressurized and the crystals were collected for analysis. The external shape of the crystals was examined by field emission scanning electron microscopy (FE-SEM, Hitachi S-4300&EDX-350). The crystal size was measured using a particle size analyzer (PSA, Ankersmid CIS-50). The crystallinity was analyzed by powder X-ray diffractometry (XRD, Rigaku D/Max-2500) at a  $2\theta$  range of 5-45°. The thermal behavior of the crystals was analyzed by differential scanning calorimetry (DSC, TA Instruments TA-400). The samples were heated from 50 to 250 °C at a heating rate of 10 °C/min.

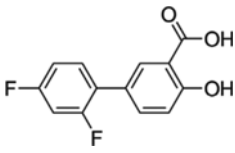
## RESULTS AND DISCUSSION

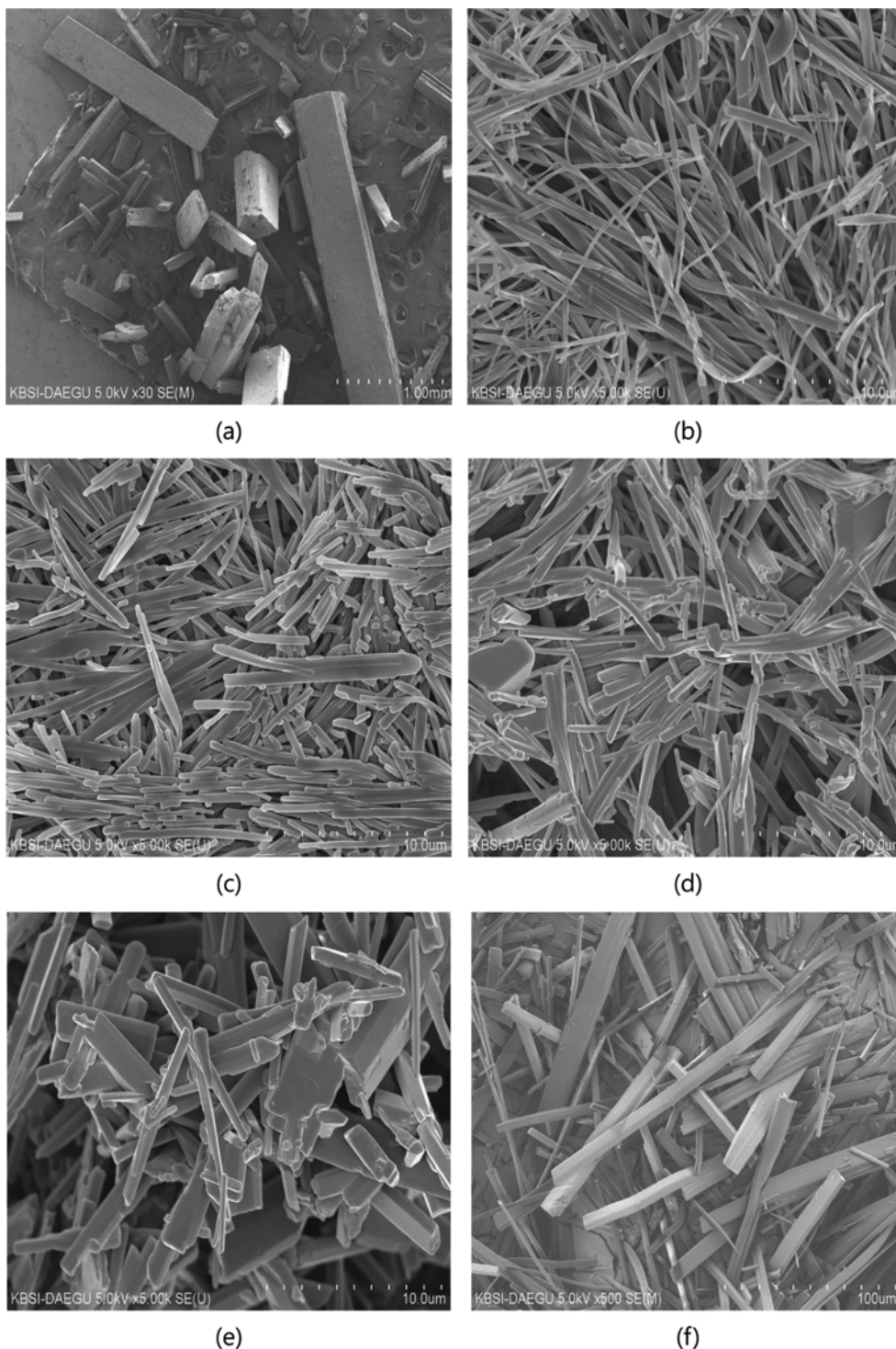
### 1. Changes in Crystal Habit

Fig. 1 shows the SEM photomicrographs of diflunisal crystals obtained in the water- and carbon dioxide-antisolvent experiments. Also shown is a photo of the raw material diflunisal crystals (Fig. 1(a)). As can be seen, the habit of the diflunisal crystals was changed depending on the experimental variables. Note that the magnification of Fig. 1(a) is  $\times 30$ , those of Figs. 1(b)-(e) are  $\times 5000$ , and that of Fig. 1(f) is  $\times 500$ . The comparison of Figs. 1(a) and 1(b) therefore shows that the size of raw diflunisal particles decreased by an order of magnitude upon crystallization. However, Fig. 1(b) also indicates that water-antisolvent crystallization produced particles exhibiting an extremely high aspect ratio, thus giving a fiber-like external shape. This is due to the rapid growth on a particular crystal face in the axial direction. Therefore, we chose to focus on crystal growth retardation in a specific direction, and attempted to minimize the particle aspect ratios.

To achieve these objectives, three experimental parameters were employed: the application of ultrasonic waves, the use of a carbon dioxide-antisolvent, and the addition of habit-modifying agents. Figs. 1(c)-(f) illustrate that such changes in experimental parameters influenced the external shape of the resulting particles. Fig. 1(c) shows the particles obtained when ultrasonic waves (5 W) were applied to the system during nucleation and crystal growth. The presence of ultrasonic waves contributed to the growth retardation of diflunisal crystals and as a result, shorter particles were ob-

**Table 1. Physicochemical properties of diflunisal**

Properties	
Chemical formula	$C_{13}H_8F_2O_3$
Chemical structure	
Molecular weight	250.19 g/mol
CAS No.	22494-42-4
Solubility	Soluble in methanol, acetone, DMF
Melting point	210-211 °C
Usage	Analgesic anti-inflammatory drug



**Fig. 1.** SEM photomicrographs of diflunisal crystals obtained using a range of experimental conditions: (a) Raw material, (b) crystallized from the water-antisolvent experiment, (c) crystallized from the water-antisolvent experiment in the presence of ultrasonic waves, (d) crystallized from the water-antisolvent experiment in the presence of sebacic acid, (e) crystallized from the water-antisolvent experiment in the presence of Span 83, and (f) crystallized from the carbon dioxide-antisolvent experiment.

served, as shown in Fig. 1(c). To explain the role of ultrasonic waves on the production of shorter particles, the concept of induction time can be used. The induction time means the elapsed time between the time of supersaturation and advent of crystals. The pres-

ence of ultrasonic waves in the solution should decrease the induction time between the phases of nucleation and crystallization. Generally, as the induction time decreases, the degree of supersaturation of the solution should increase. As a result, the presence of

ultrasonic waves causes a higher degree of supersaturation in the drug solution, and therefore, a larger number of nuclei could be formed, which leads to the smaller particle size. In addition, the ultrasonic waves can contribute to the particle breakage.

Figs. 1(d) and 2(e) show the crystals obtained when sebacic acid and Span 83 were added to the system, respectively. The two habit-modifying agents lowered the aspect ratio of the diflunisal particles and induced the change of the crystal habit from acicular to particulate. The role of Span 83 as a growth retardant appeared to be greater than that of sebacic acid. Furthermore, Fig. 1(f) shows the typical shape of diflunisal particles obtained from the carbon dioxide-antisolvent experiment. As mentioned, the magnification of Fig. 1(f) ( $\times 500$ ) is an order of magnitude smaller than that of photos shown in Figs. 1(b)-(e) ( $\times 5000$ ). This means that the particles shown in Fig. 1(f) are ten-times larger than those in Figs. 1(b)-(e). Comparison of Figs. 1(b) and 1(f) illustrates that changing the antisolvent from water to carbon dioxide significantly changes the crystal habit. Crystals obtained from the water-antisolvent experiments exhibited fiber-like shapes, while those produced from the carbon dioxide-antisolvent experiments exhibited columnar shapes. In addition, the crystals obtained from the carbon dioxide-antisolvent experiments were an order of magnitude larger than those produced from the water-antisolvent experiments, as shown in Fig. 1(f).

It can be expected that the changes in crystal habit may due to the appearance of new polymorphs of diflunisal crystals upon the use of ultrasonic waves, carbon dioxide-antisolvent and habit-modifying agents. In general, it is possible that different polymorph of diflunisal can exhibit different crystal habits. In this paper, however, it was difficult to directly relate the change in crystal habit to the polymorphic change (structural modification) of a crystal. Thus, it was difficult to verify the relation between the external shape (habit) and the internal structure (polymorph) of diflunisal particles. In addition, the evidence of formation of a new polymorph should be verified using additional analytical instruments, which was not performed in this work. Therefore, in this investigation,

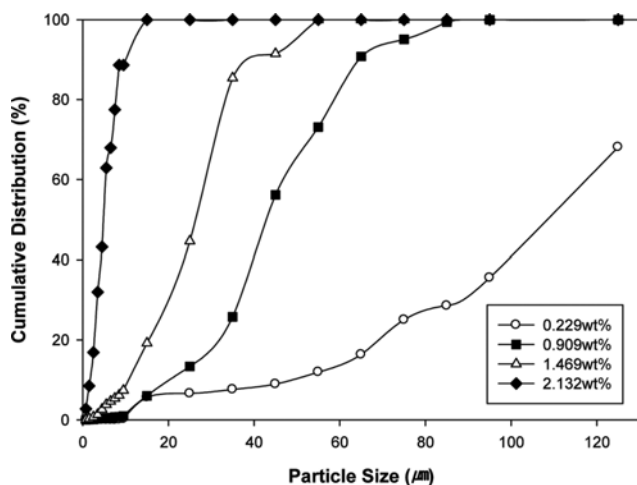


Fig. 2. Particle size distribution of diflunisal from the water-antisolvent experiments in the presence of sebacic acid at various concentrations.

the possible polymorphic change of diflunisal crystal was limitedly mentioned. Instead, we emphasized the issue of growth retardation can explain the habit modification of diflunisal.

In our investigation, the supersaturation of crystallizing solutions was not measured because we presumed that the supersaturation was almost constant in all the crystallization experiments. In our study, the variation ranges of experimental conditions (concentration, temperature and amount of solution used etc.) were not very large so that it could be considered that the supersaturation remained constant.

## 2. Particle Size and Aspect Ratio

Fig. 2 shows the effect of sebacic acid concentration (0.229–2.132 wt%) on the particle size distribution of diflunisal obtained from the water-antisolvent experiments. Sebacic acid appeared to retard the fibrous crystal growth of diflunisal and shorten its length. As the concentration of sebacic acid was increased from 0.229 to 2.132 wt%, the overall particle size decreased. In fact, due to their irregular shape, it may be difficult to accurately represent the particle size of the fibrously shaped crystals as shown in the SEM images of Fig. 1. However, the principle of particle size measurement is counting the average time taken for a laser beam to pass through a

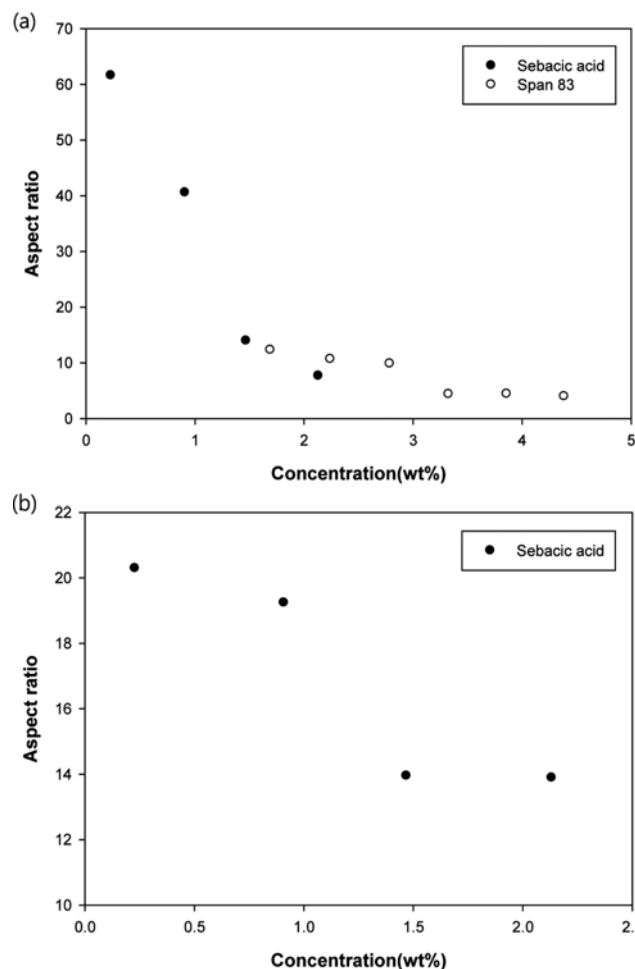


Fig. 3. Aspect ratio of diflunisal crystals as a function of concentration of habit-modifying agents in the (a) water-antisolvent experiments, and (b) carbon dioxide-antisolvent experiments.

particle in a vigorously agitated vessel. Therefore, the particle sizes shown in Fig. 2 may reflect the average size or length of the fiber-like diflunisal particles.

Fig. 3 shows the aspect ratio (length : width ratio) of diflunisal particles produced from the water- (Fig. 3(a)) and carbon dioxide-antisolvent (Fig. 3(b)) experiments. In this study, the aspect ratio was estimated by measuring the dimensions of 100 sample particles observed by SEM and taking an average of their ratios. In Fig. 3, the aspect ratio of the diflunisal crystals is presented as a function of habit-modifying agent concentration. In the water-antisolvent experiments, both sebacic acid and Span 83 were employed, whereas in the carbon dioxide-antisolvent experiments, only sebacic acid was utilized. Generally, the aspect ratio of the diflunisal particles was reduced with an increase in concentration of the habit-modifying agents. In the water-antisolvent experiments (Fig. 3(a)), an increase in the sebacic acid concentration from 0.229 to 2.132 wt% lowered the aspect ratio from 62 to 8.5, while an increase in Span 83 concentration from 1.712 to 4.415 wt% lowered the aspect ratio from 11 to 4.0. Similarly, in the carbon dioxide-antisolvent experiments (Fig. 3(b)), an increase in sebacic acid concentration from 0.229 to 2.132 wt% lowered the aspect ratio from 21 to 14. In addition, the influence of sebacic acid on the aspect ratio was greater when water was used as an antisolvent. Indeed, the aspect ratio of particles produced from the carbon dioxide-antisolvent experiments was significantly smaller than those from the water-antisolvent experiments in the absence of additives. Overall, the results obtained from the particle size and aspect ratio analysis of the diflunisal particles revealed that sebacic acid and Span 83 successfully play a role as growth retardants for the crystallized particles.

From the measurement of aspect ratio of diflunisal crystals, we observed that the presence of sebacic acid clearly induced the shortening of crystal length. This means that the sebacic acid can prevent the rapid growth of crystal only along the axial direction so that the crystal can be shortened. The presence of sebacic acid on the crystal growing surface of crystals may prevent the mass transfer of diflunisal molecules from reaching to the growing lattice, and eventually the crystal growth along a particular direction can be retarded. And as a result, the aspect ratio could be reduced.

Indeed, to fully explain the growth retardation, the molecular behavior of sebacic acid on the crystal growing surface of diflunisal particles should be described in detail. However, this kind of approach is beyond the limit of our research facility, and therefore explanations based only on the experimental results have been given in this paper. We regard that the result that showed the shortening of crystal length can reflect the role of sebacic acid as a growth retarding agent.

In regards to the reduction of particle aspect ratio, another explanation is possible which considers the enhanced nucleation caused by the presence of additive. Indeed, the shortening of crystal length may possibly be the outcome of additive-assisted enhanced nucleation. If an additive favors nucleation, more nuclei or crystals are created, leading to a lower solution concentration which limits the development of the formed crystals and therefore, smaller crystals are obtained.

### 3. Thermal Analysis

The thermal behavior of the diflunisal crystals was determined

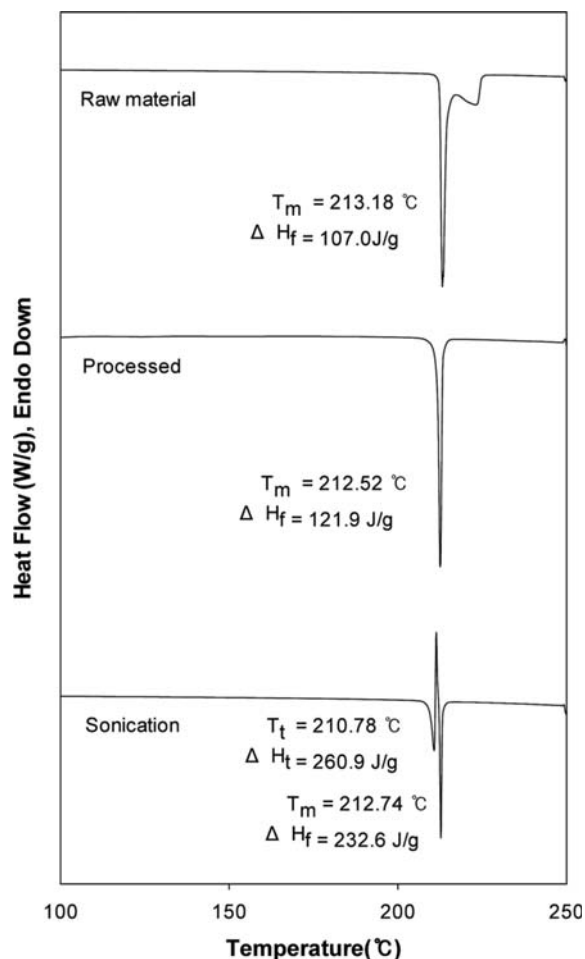


Fig. 4. DSC curves of diflunisal particles produced from the water-antisolvent experiments.

using DSC measurements. Fig. 4 shows the DSC curves of three diflunisal samples: the as-received particles (raw material), crystals from the water-antisolvent experiment in the absence of habit-modifying agents and external disturbances (processed), and crystals from the water-antisolvent experiments where ultrasonic waves were applied (sonication). Overall, different DSC patterns were obtained according to the different process conditions employed. However, all three samples exhibited identical melting temperatures ( $T_m$ ) of  $\sim 212^\circ\text{C}$ . In the DSC curve of the raw diflunisal, two endothermic peaks were observed: a major melting peak followed by a small endothermic peak at the tail of the curve. This pattern implies that two phase transitions occurred during fusion of the as-received diflunisal sample. The appearance of two phase transition curves for the as-received sample could be explained by the possible presence of a partly different crystalline form in the crystalline structure of raw material sample. The XRD pattern of raw material in Fig. 6 could be an additional evidence of the presence of different crystalline form inside the crystal (please see the appearance of a major peak at  $2\theta$  of  $42^\circ$ ). In contrast, the processed diflunisal sample showed only a single endothermic peak at  $T_m=212.52^\circ\text{C}$  [11]. In addition, the heat of fusion ( $\Delta H_f=121.9\text{ J/g}$ ) of the processed crystal was higher than that of the raw material ( $\Delta H_f=107.0\text{ J/g}$ ).

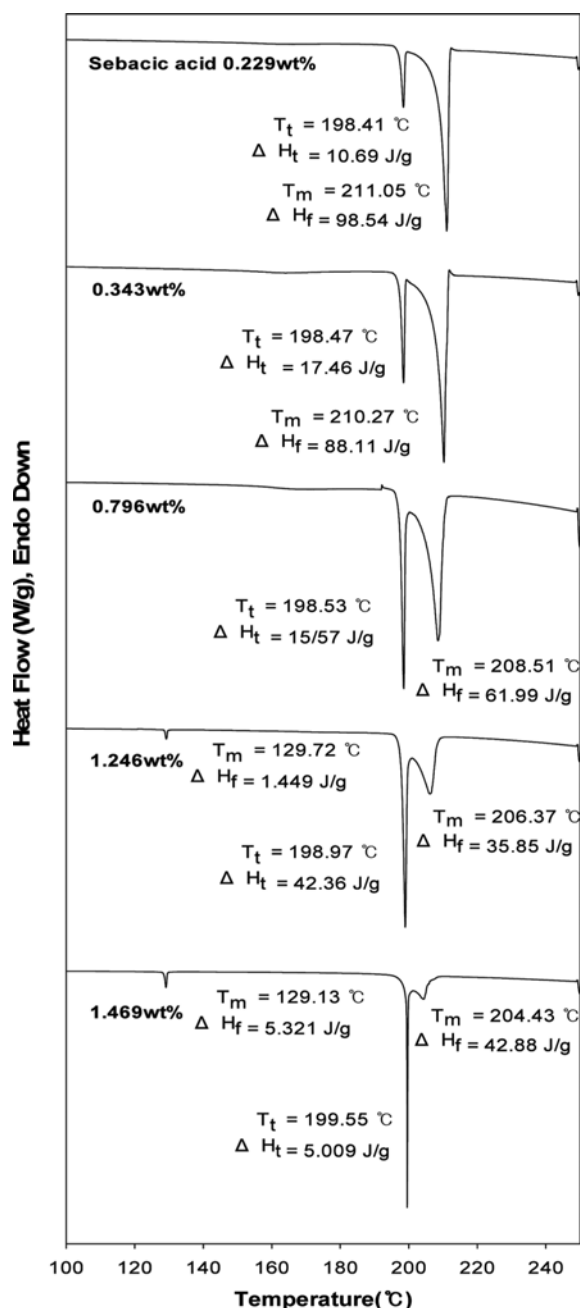


Fig. 5. DSC curves of diflunisal particles obtained from the water-antisolvent experiments employing sebacic acid at various concentrations.

Interestingly, the diflunisal samples produced in the presence of ultrasound displayed a quite different DSC pattern, with two types of phase transitions occurring with an increase in temperature. First, an endothermic solid-phase transition peak was observed at  $T_t=210.78$  °C (with a heat of transition  $\Delta H_t=260.9$  J/g), followed by a sharp exothermic recrystallization peak. Finally, an endothermic melting peak appeared at  $T_m=212.74$  °C (with a heat of fusion  $\Delta H_f=232.6$  J/g). These results imply that the presence of ultrasonic waves may modify the melting behavior of diflunisal crystals, including the mechanism of melting and the heat of fusion [12]. There-

Table 2. Transition temperature ( $T_t$ ), heat of transition ( $\Delta H_t$ ), melting temperature ( $T_m$ ) and heat of fusion ( $\Delta H_f$ ) of DSC curves in Fig. 6

Sebacic acid concentration (wt%)	$T_t$ (°C)	$\Delta H_t$ (J/g)	$T_m$ (°C)	$\Delta H_f$ (J/g)
0.229	198.41	10.69	211.05	98.54
0.343	198.47	17.46	210.27	88.11
0.796	198.53	15.57	208.51	61.99
1.246	198.97	42.36	206.37	35.85
1.469	199.55	50.09	204.43	42.88

fore, it is presumed that a metastable form could have crystallized in the presence of ultrasonic waves.

Fig. 5 shows the DSC curves of processed diflunisal crystals in the presence of sebacic acid at various concentrations (0.229-1.469 wt%). In all DSC curves, two endothermic peaks were observed at two different temperatures, corresponding to the phase transition of the diflunisal particles. Table 2 summarizes the values for the transition temperature ( $T_t$ ), heat of transition ( $\Delta H_t$ ), melting temperature ( $T_m$ ) and heat of fusion ( $\Delta H_f$ ) of DSC curves in Fig. 5. With a sebacic acid concentration of 0.229 wt%, the first and second peaks were observed close to 198 and 211 °C, respectively. As the concentration of sebacic acid increased (up to 1.469 wt%), the temperature at which the first peak appeared was relatively constant (198 °C), while the temperature at which the second peak appeared decreased to 204 °C. Thus, at a sebacic acid concentration of 0.229 wt%, the two endothermic peaks were distinctly separated, and as the concentration increased, the two peaks began to merge. In addition, as the sebacic acid concentration increased, the heat of fusion of the first peak increased, while that of the second peak decreased. Comparison of the DSC curves in Figs. 4 and 5 shows that the presence of a high concentration of sebacic acid may reduce the melting point of diflunisal particles from 212 to 199 °C. Observation of the DSC curves at sebacic acid concentrations of 1.246 and 1.469 wt% revealed small peaks at 129.72 and 129.13 °C, respectively, that may correspond to the melting of sebacic acid. Thus, at high sebacic acid concentrations, the sebacic acid also precipitated from the solution upon mixing with the antisolvent, and was present as a mixture with diflunisal in the resulting particles. However, at this stage in the investigation, it is difficult to identify whether the sebacic acid was incorporated inside the crystal or was present on the precipitated diflunisal particle surfaces.

#### 4. XRD Analysis

Information relating to the crystallinity of a particle can be obtained from XRD analysis. Fig. 6 shows the XRD patterns of the as-received diflunisal (raw material) along with those of four diflunisal samples obtained using different experimental conditions. The XRD pattern of particles obtained from the water-antisolvent experiments (processed) exhibited a different pattern to the raw material, demonstrating that the diflunisal crystalline structure was somewhat modified upon crystallization using the water-antisolvent. The XRD pattern of particles obtained from the water-antisolvent experiments with the application of ultrasonic waves is also shown, suggesting that the presence of ultrasound did not affect the XRD pattern of the diflunisal particles. As mentioned, ultra-

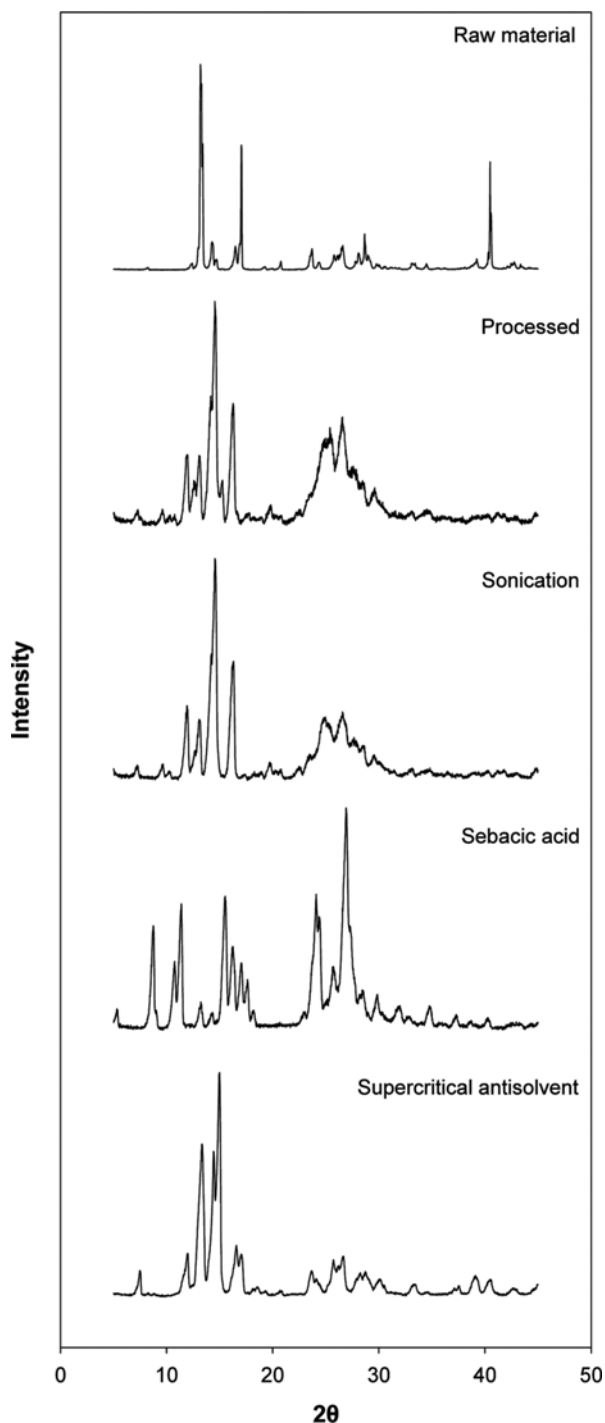


Fig. 6. XRD patterns of diflunisal particles produced from the water and carbon dioxide-antisolvent experiments.

sonic waves did modify the thermal behavior (DSC pattern) of the crystals. The XRD pattern obtained from water-antisolvent experiments in the presence of sebacic acid (sebacic acid) gave a contrasting result. This suggests that the externally added material strongly influenced the crystalline structure of diflunisal particles, while disruption by ultrasonic waves had little effect. Finally, Fig. 6 shows the XRD pattern of diflunisal particles produced from the carbon dioxide-antisolvent experiments (supercritical antisolvent).

Comparison of this XRD pattern with the “processed” pattern revealed that the type of antisolvent (water or carbon dioxide) had no significant effect on the crystallinity of diflunisal particles. It is noteworthy that the change in antisolvent from water to carbon dioxide caused growth retardation of the particles, but barely affected the internal structure of the crystals.

## CONCLUSIONS

Diflunisal was recrystallized from acetone solution using two different antisolvents. Diflunisal particles with very high aspect ratios were produced from both antisolvent experiments. The growth of these particles was retarded by applying ultrasonic waves and by adding habit-modifying agents (sebacic acid and Span 83). The use of ultrasonic waves induced the production of shorter particles. Furthermore, with an increase in concentration of sebacic acid and Span 83 in the system, the aspect ratio of the diflunisal crystals decreased significantly. DSC analysis revealed that the thermal behavior of the as-received diflunisal particles was altered by the antisolvent recrystallization. Finally, XRD analysis also showed that the presence of ultrasound and external additives modified the internal crystalline structure as well as the external crystal habit.

## ACKNOWLEDGEMENTS

This research was supported by Basic Science Research Program through the National Research Foundation of Korea (NRF) funded by the Ministry of Education (2017R1D1A3B05030114).

## REFERENCES

1. V. Prosapio, E. Reverchon and I. De Marco, *J. Supercrit. Fluids*, **107**, 106 (2016).
2. I. A. Cuadra, A. Cananas, J. A. R. Cheda, F. J. Martinez-Casado and C. Pando, *J. CO<sub>2</sub> Utiliz.*, **13**, 29 (2016).
3. C. Neurohr, M. Marchivie, S. Lecomte, Y. Cartigny, N. Couvrat, M. Sanselme and P. Subra-Paternault, *Cryst. Growth Des.*, **15**, 4616 (2015).
4. W. Kaiyaly, H. Larhrib, B. Chikwanha, S. Shojaee and A. Nokhodchi, *Int. J. Pharm.*, **464**, 53 (2014).
5. S.-J. Park and S.-D. Yeo, *J. Supercrit. Fluids*, **47**, 85 (2008).
6. A. S. Myerson, *Handbook of Industrial Crystallization*, 2<sup>nd</sup> Ed., Chapter 3, Butterworth Heinemann, Boston (2002).
7. G. M. Van Rosmalen, *J. Cryst. Growth*, **99**, 1053 (1990).
8. C. Thompson, M. C. Davies, C. J. Roberts, S. J. B. Tendler and M. J. Wilkinson, *Int. J. Pharm.*, **280**, 137 (2004).
9. M. L. Cotton and R. A. Hux, *Analyt. Profil. Drug Subst.*, **14**, 491 (1985).
10. G. Giammona, G. Cavallaro, G. Pitarresi, C. Ventura and S. Palazzo, *Int. J. Pharm.*, **105**, 57 (1994).
11. M. C. Martinez-Oharriz, C. Martin, M. M. Goni, C. Rodriguez-Espinosa, M. C. Tros De Ilarduya-Apaolaza and M. Sanchez, *J. Pharm. Sci.*, **83**, 174 (1994).
12. J. L. Ford and P. Timmins, *Pharmaceutical Thermal Analysis*, Ellis-Horwood Ltd., Chichester, U.K. (1989).